Graphite Layer Nano-Composites with Polyurethane Matrix

Michael Czajka and Robert A. Shanks

School of Applied Sciences, RMIT University
Box 2476 GPO, Melbourne, VIC 3001, Australia
Tel. 613 9925 2122, Fax 613 9925 3747, e-mail: robert.shanke@rmit.edu.au

ABSTRACT

Expanded graphite oxide (EGO) composites were prepared in a crosslinked polyether–polyurethane (PU). EGO was of low bulk density, though it was uniformly dispersed in the polyol by ultrasonication prior to diisocynate chain extension and crosslinking. The EGO–PU composites were characterised using electron microscopy, X-ray scattering and thermogravimetry. Mechanical properties where measured using a multiplexed frequency modulated force that enable calculation of activation energy of the glass transition. Activation energy increased with EGO content, damping of the PU was decreased, creep was significantly reduced and the limited recovery was retarded.

Keywords: advanced materials, graphite nano-structures, expanded graphite oxide, thermomechanical properties

1 INTRODUCTION

Graphite oxide intercalation compound is formed by oxidation of graphite, in for example sulfuric–nitric acid mixture. Graphite oxide is expanded into individual sheets by rapidly heating. Graphene is formed by reduction of graphite oxide with reagents such as hydrazine, however aqueous conditions are required. Graphene can be formed by direct delamination of graphite with adhesive tape, though the route via graphite oxide is a preferred preparative method. Graphene only has surfaces; there is no bulk structure, that is all atoms are at an interface. This makes graphene unstable because of its high surface energy [1,2]. Graphene has an extremely high modulus, of the order of 1 TPa, and conductivity greater that copper. Graphene can be stabilized by dispersion in a polymer, such as a polysiloxane [3] or using a polymer latex [4].

Graphite oxide and graphene can be dispersed into thermoplastics to give nano-composites with novel properties at relatively low filler concentrations [5,6]. Properties obtained from graphene oxide and graphene nano-composites include conductivity, enhanced thermal stability and increased modulus and strength. The dispersing polymer can be a thermoplastic [7], using either melt or solution dispersion, or a thermosetting polymer, such as an epoxy resin [8]. Graphite oxide layers have high modulus and tensile strength, while introducing conductivity to their composites due to a low percolation threshold.

The aim was to prepare expanded graphite oxide and disperse it in a polyurethane formed from a polyol (poly(oxypropylene glyceride). An important criteria compared with solution preparations was to prevent agglomeration of the graphite oxide after dispersion, before gelation of the polymer. Characterisation of the nano-composites was performed to determine contribution of expanded graphite oxide to a moderately damping elastomer.

2 EXPERIMENTAL

2.1 Materials

Methane 4,4'-diphenyldiisocyanate (MDI), number 7114 with functionality 2.2, was obtained from Huntsman Chemicals, Australia Ltd. The polyol was Voranol 3010 (V3010, Dow Chemicals), a propoxylated glycerol with an average of 45 propoxy groups per mole of glycerol. V3010 was dried using molecular sieve (type 3A) prior to use to avoid foaming of the PU due to reaction of water with MDI. Graphite oxide (GO) was obtained from Graftech Inc. GO was expanded (EGO) by heating rapidly to 800 °C. This temperatue was greater than the recommended temperature at which expansion will occur (about 260 °C), however rapid expansion provided more complete exfoliation.

2.2 Expanded Graphite–Polyurethane Composite Preparation

Dispersion of EGO was by ultrasonication for 4 min. The polyol with dispersed EGO was chain extended and crosslinked with methane 4,4'-diphenyldiisocyanate (MDI) to form a poly(ether-urethane) (PU). EGO concentrations of 0.5 and 1.0 %·w/w were prepared. Graphite oxide was preferred to disperse in the polyol component since both are polar and the polyol is the non-reactive PU component. The polyol–EGO dispersions were mixed with MDI, spread on a metal plate with spacer plate lined with polyethylene film, to give sheets of about 1.5 mm thickness and cured in an oven at 60 °C for 4 h. The composites were stored in zip-lock polyethylene bags prior to testing.

2.3 Composite Characterisation

The GO-PU composites were analysed using field-emission scanning electron microscopy (FEI Quanta 200

ESEM), wide-angle X-ray scattering (Bruker Discover 8, powder camera) and thermogravimetry (Perkin-Elmer Pyris 1 TGA, 30 to 850 °C at 10 °C·min^{-1} under a nitrogen purge of 20 mL·min^{-1} until 700 °C when the purge gas was changed to air.

2.4   Mechanical Property Evaluation

Characterisation of mechanical properties was performed with stress-strain analysis (tensile mode, 10 mm·min^{-1}, Instron 4065), creep and recovery (tensile mode, static strain, TA Instruments Q800) with a force of 0.1 N for 30 min followed by recovery from 120 min. Modulated force thermomechanical (mf-TM) analysis (Perkin-Elmer Diamond DMA, using a multiplexed synthetic frequency containing 1, 2, 4, 10, 20 Hz, with 10 μm deformation, -60 to +120 °C at 2 °C·min^{-1}).

3   RESULTS AND DISCUSSION

SEM showed relatively uniform exfoliation of graphite oxide sheets with some residual unexfoliated graphite oxide. Figure 1 shows graphite oxide and Figure 2 expanded graphite oxide sections, the latter while expanded still contained connected sheets that were ultrasonically disrupted during dispersion into the polyol. Some detachment of sheets is shown in GO (Figure 1) resulting from the oxidation treatment. Rapid expansion by suddenly heating to high temperature gave about 100–200 fold increase in bulk volume. X-ray data showed a single sharp diffraction peak for unexfoliated graphite at a scattering angle of 26° in both GO and EGO, though with much reduced intensity in the latter.

Thermogravimetry (figure not shown in this paper) demonstrated that the thermal stability of the PU was increased by GO. The increased thermal stability was due to retardation of volatile emissions by tortuous paths created by GO and absorption of both polymer and degradation products by GO. The modulus and yield strength of GO-PU nano-composites were increased, while the elongation at break was reduced.
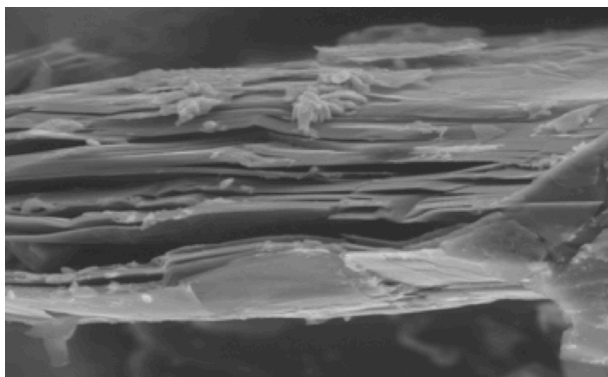

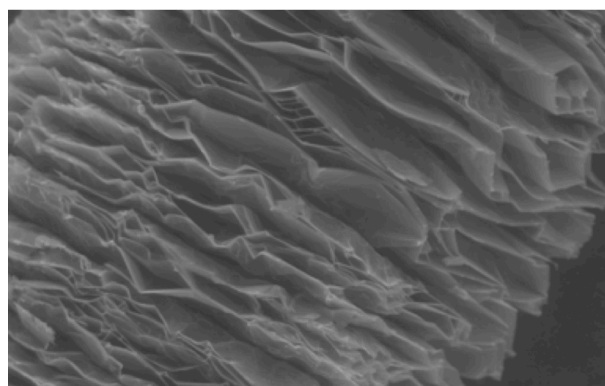Figure 1: Graphite oxide before thermal expansion.

Figure 2: Graphite oxide after thermal expansion

PU creep (Figure 3) was significantly reduced by EGO, while recovery was slowed and the non-exponentiality (skewness of the exponential recovery curve) increased consistent with a greater distribution of relaxation times. The main constraint of EGO on the creep curve was in the elastic regime where extension under the same stress was about half. The viscoelastic and viscous creep regions were similar with and without EGO. The relaxation curves mirrored the creep response with viscoelastic recovery curves parallel. Permanent set was reduced in the EGO composites, though not in the order of EGO composition, which may be due to difference in the viscous part of the creep rather than recovery ability.
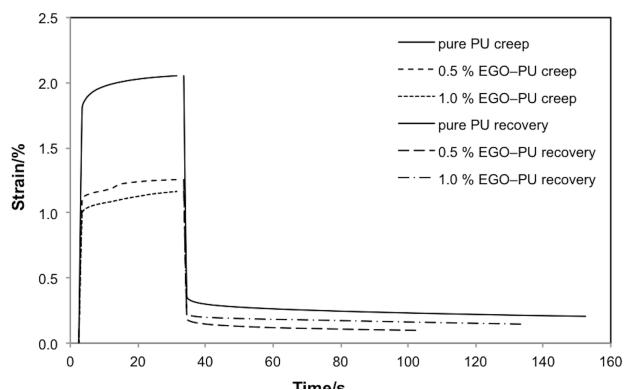

Figure 3: Creep and recovery curves for pure PU and nano-composites with 0.5 and 1.0 % EGO

Results for mf-TM of pure PU are shown in Figure 4. Storage modulus, loss modulus and tan(δ) are plotted with each data set showing a shift to higher temperatures with incremental increas in frequency. The storage modulus in the glassy and rubbery regions was increased with PU-EGO, while the damping factor was decreased. The glass transition of the flexible polyol phase was not significantly changed. Elastic (storage modulus) properties are predominant except in the transition region, with tan(δ) maxima from -30 to -15 °C, where tan(δ) approaches 1.0 with equal elasticity and viscoelasticity, a highly damping material.

The change in storage modulus from the glassy state at 13-16 GPa to about 10 GPa about Tg near 100 °C, that is about 1000 fold was consistent with the mainly amorphous elastomeric structure, interrupted only by the dispersed urethane hard phase. This large modulus change was a challenge for the instrument when five frequencies were being measured because the synthetic frequency mode increases the total force required when the frequency maxima randomly coincide, which required a force close to the instrument maximum.
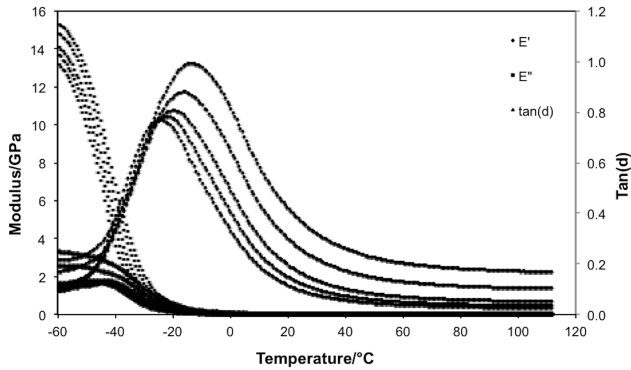

Figure 4: Storage modulus, loss modulus and damping factor of the unfilled PU measured at five frequencies.

Figures 5 and 6 show the mf-TM curves for the composites with 0.5 and 1.0 %·w/w EGO respectively. Figures 5 and 6 are plotted on the same scale as Figure 4 for direct comparison. The elastic modulus at low temperature for each EGO concentration was decreased. Reinforcement by EGO is not expected in the glassy state since the PU is brittle in this temperature range. Defects in the matrix phase may be introduced by EGO decreasing elastic modulus. This may be apparent in the failure of the 0.5 %·w/w composite at 60 °C, several scans were performed with similar results, though the 1.0 %·w/w composite remianed intact at the finish of several scans. Tha damping fctor was reduced to a maximum of 0.8 in each of the EGO composites. Filler caused the composite to become more elastic than the pure PU.
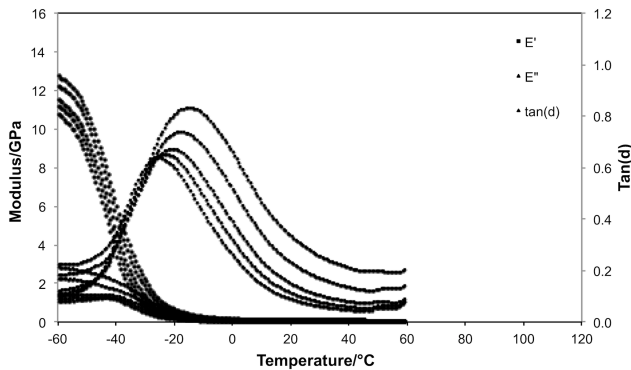

Figure 5: Storage modulus, loss modulus and damping factor of PU with 0.5 % EGO measured at five frequencies.
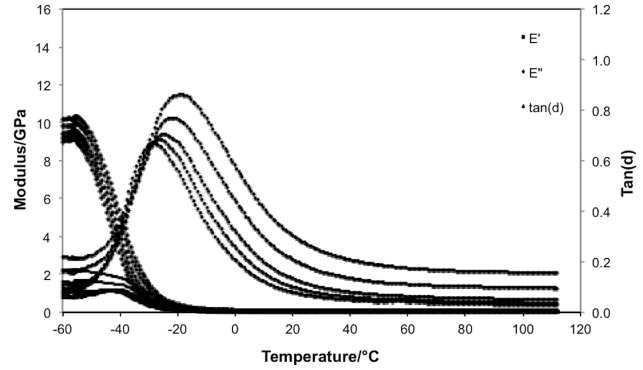

Figure 6: Storage modulus, loss modulus and damping factor of PU with 1.0 % EGO measured at five frequencies.

The viscoelasticity (loss modulus) was decreased even more than the storage modulus in the composites. Filler is expected to decrease flow-like character by imobilizing the moelcules. The changes to modulated force properties brought about by EGO should be considered in the context that the measuremnts were performed in the viscoelastic range with a constant deformation of ±10 μm. The small deformations have revealed EGO contributions through decrease of glassy state storage modulus and transition stae damping properties.

Synthetic multiplexed frequency data for the tan(δ) peak temperature at each frequency was used to calculate an Arrhenius activation energy (E_a) for each composition. The peak maximum temperature for tan(δ), converted to reciprocal absolute temperature (1/K) was plotted with the logarithm of the respective applied frequency. The gradient of the line of best fit is $-E_a/R$ (the gas constant, R = 3.182 J/K·mol). The Arrhenius plots are shown in Figure 7. The pure PU gave E_a = 61 kJ/mol·K, with 0.5 %·w/w EGO E_a = 65 kJ/mol·K and with 1 %·w/w EGO E_a = 70 kJ/mol·K. Thus the activation energy for the glass transition according to the tan(δ) peak increased slightly with EGO content.
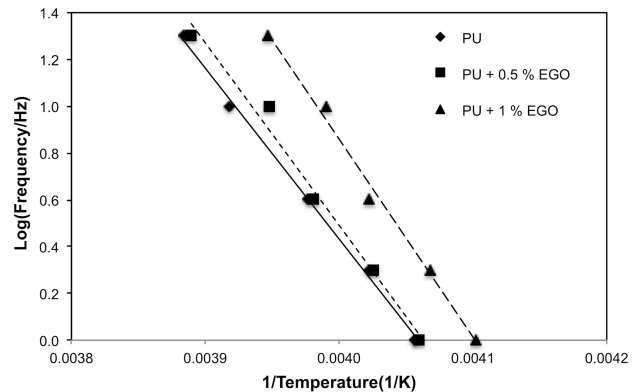

Figure 7: Arrhenius plots from multifrequency mf-TM.

The relatively low concentrations of EGO caused significant change in mechanical properties under high strains experienced in creep and recovery measurements. Adsorption and binding of PU molecules by the molecularly thin yet broad EGO sheets was revealed under the high strain conditions. Both the creep and recovery parts of the experiment were effected by presence of EGO in contrast to the mf-TM measurements made within the linear viscoelasticy region where structures and interactions suffer minimal disturbance by the measurement.

Preparation of the PU with EGO dispersed in-situ in the polyol was suitable for the ultra-low bulk density EGO flakes. The composite presented in this paper were made immediately after expansion of GO to minimize absorption of water or orther impurities by the EGO. However, other preparations were satisfactorily prepared using stored EGO. Higher concentrations of EGO can be obtained since the viscosity of the EGO–polyol dispersion was not too high for mixing with MDI and casting a sheet. A limitation on high EGO concentrations is the tendency to agglomerate after dispersion and before gelation of the crosslinking PU.

4 CONCLUSION

Crosslinked polyether–polyurethane nano-composites were prepared from expanded graphite oxide (EGO) by dispersing EGO in the polyol then crosslinking with MDI. GO was rapidly expanded at high temperature and the low bulk density EGO was readily dispersed in the polyol using ultrasonication.

The dispersion and crosslinking processes were able to prevent agglomeration of EGO and form uniform composites with modification of PU damping properties. Small shifts in glass tranistion tmeperature were observed, resulting in an incremental increase in transition activation energy. Damping was reduced with increasing EGO concentration. Creep and recovery were significantly inhibited since the reinforcing action of EGO was more apparent under high strain conditions. Further studies of PU–EGO nano-composites will include extending the range of EGO concentrations, mf-TM over an extended frequency range for preparation of time–temperature–superposition mastercurves and measurement of the electrical conductivity under static and strained conditions.

REFERENCES

[1] C.N.R. Rao, K. Biswas, K.S. Subrahmanyam and A. Govindaraj, Graphene, the new nanocarbon, J. Mat. Chem., **19**, 2457-2469 (2009).

[2] K.P. Loh, Q. Bao, P.K. Ang and J. Yang, The chemistry of graphene, J. Mat. Chem., **20**, 2277-2289 (2010).

[3] R. Verdejo, F. Barroso-Bujans, M.A. Rodriguez-Perez, J.A.d. Saja and M.A. Lopez-Manchado, Functionalized graphene sheet filled silicone foam nanocomposites, J. Mat. Chem., **18**, 2221-2226 (2008).

[4] R. Wissert, P. Steurer, S. Schopp, R. Thomann and R. Mülhaupt, Graphene Nanocomposites Prepared From Blends of Polymer Latex with Chemically Reduced Graphite Oxide Dispersions, Macromol. Mat. Eng., **295**, 1107–1115 (2010).

[5] P. Steurer, R. Wissert, R. Thomann and R. Mülhaupt, Functionalized Graphenes and Thermoplastic Nanocomposites Based upon Expanded Graphite Oxide, Macromol. Rapid Comm., **30**, 316-327 (2009).

[6] F.T. Cerezo, C.M.L. Preston and R.A. Shanks, Structural, mechanical and dielectric properties of poly(ethylene-co-methyl acrylate-co-acrylic acid) graphite oxide nanocomposites, Comp. Sci. and Tech., **67**, 79-91 (2007).

[1] F.T. Cerezo, C.M.L. Preston and R.A. Shanks, Morphology, thermal stability, and mechanical behavior of [poly(propylene)-grafted maleic anhydride]-layered expanded graphite oxide composites, Macromol. Mat. and Eng., **292**, 155-168 (2007).

[8] O. Ozcelik, L. Aktas, and M. C. Altan, Thermo-oxidative degradation of graphite/epoxy composite laminates: Modeling and long-term predictions, eXPRESS Polym. Lett., **3**, 797–803 (2009).